Published in final edited form as:
Circulation. 2008 November 4; 118(19): 1953–1960. doi:10.1161/CIRCULATIONAHA.108.789743.

Molecular Imaging of Activated Matrix Metalloproteinases in Vascular Remodeling

Jiasheng Zhang, M.D., **Lei Nie, Ph.D.**, **Mahmoud Razavian, Ph.D.**, **Masood Ahmed, M.D.**, **Lawrence W. Dobrucki, Ph.D.**, **Abolfazl Asadi, Ph.D.**, **D. Scott Edwards, Ph.D.**, **Michael Azure, Ph.D.**, **Albert J. Sinusas, M.D.**, and **Mehran M. Sadeghi, M.D.**
Raymond and Beverly Sackler Cardiovascular Molecular Imaging Laboratory, Section of Cardiovascular Medicine (J.Z., L.N., M.R., M.A., L.W.D., A.A., A.J.S., M.M.S.), Yale University School of Medicine, New Haven, CT 06520, VA Connecticut Healthcare System (J.Z., L.N., M.R., M.A., A.A., M.M.S.), West Haven, CT 06516 and Lantheus Medical Imaging (S.E., M.A.), North Billerica, MA

Abstract

Background—Matrix metalloproteinase (MMP) activation plays a key role in vascular remodeling. RP782 is a novel ^{111}In –labeled tracer with specificity for activated MMPs. We hypothesized that RP782 can detect injury-induced vascular remodeling in vivo.

Methods and Results—Left common carotid artery injury was induced using a guide wire in apolipoprotein $E^{-/-}$ mice. Sham surgery was performed on the contralateral artery, which served as control for imaging experiments. Carotid wire injury led to significant hyperplasia and expansive remodeling over a period of 4 weeks. MMP activity detected by in-situ zymography, increased in response to injury and was maximal by 3-4 weeks after injury. RP782 (11.1 MBq) was injected intravenously to apolipoprotein $E^{-/-}$ mice at 1, 2, 3, and 4 weeks after left carotid injury. MicroSPECT imaging was performed at 2 hours and was followed by CT angiography to localize the carotid arteries. In vivo images revealed focal uptake of RP782 in the injured carotid artery at 2, 3 and 4 weeks. Increased tracer uptake in the injured artery was confirmed by quantitative autoradiography. Pretreatment with 50-fold excess non-labeled tracer significantly reduced RP782 uptake in injured carotids, demonstrating uptake specificity. Weekly changes in the vessel wall area closely paralleled and correlated with RP782 uptake (Spearman r=0.95, p=0.001).

Conclusions—Injury-induced MMP activation in the vessel wall can be detected by RP782 microSPECT/CT imaging in vivo. RP782 uptake tracks the hyperplastic process in vascular remodeling, and provides an opportunity to track the remodeling process in vivo.

Keywords

Imaging; Metalloproteinases; Remodeling

Introduction

Vascular disease remains a major cause of morbidity and mortality in developed, and increasingly, developing countries. Advances in vascular biology in the past two decades have

Corresponding Author: Mehran M. Sadeghi, M.D., VA Connecticut Healthcare System, 950 Campbell Avenue, 111B, West Haven, CT 06516, Fax: 203-937 3884, Phone: 203-932 5711 x3398, Mehran.sadeghi@yale.edu.

Disclosures: DSE and MA are employees of Lantheus Medical Imaging. AJS and MMS receive experimental tracers from Lantheus Medical Imaging. In addition, AJS has received research grants from Lantheus Medical Imaging.

translated into the discovery of novel therapies, which have in turn, led to a reduction in morbidity and mortality. It is well-recognized that the lack of in vivo imaging modalities for detection of molecular events in the vessel wall has limited vascular biology research and the ability to detect early, presumably easier to treat, vascular disease. Molecular imaging, targeted at biologically relevant molecules or markers of vascular disease provides an opportunity to study pathogenesis, detect early disease, and track therapeutic interventions.

Matrix metalloproteinases (MMPs) are a multi-gene family of endopeptidases that play a key role in normal vascular homeostasis and pathogenesis [1, 2]. Expression, activation, and inhibition by tissue inhibitor of matrix metalloproteinases (TIMPs) are the main regulatory mechanisms of MMP activity. Imaging MMP activation can provide novel insight into the pathogenesis of vascular disease and serve as a clinical tool for tracking vascular pathology. Here, we demonstrate the feasibility of MMP-targeted in vivo hybrid imaging of vascular remodeling, a common feature of many vasculopathies, including in-stent restenosis, graft arteriosclerosis, and aneurysm formation. RP782, an ^{111}In-labeled tracer with specificity for activated MMPs [3], is used to detect injury-induced MMP activation in murine carotid arteries. High resolution imaging with accurate localization of the target artery is achieved through microSPECT imaging in combination with CT angiography. Finally, the biological significance of RP782 uptake in injury-induced vascular remodeling is addressed.

Methods

Reagents

Reagents were from Sigma (St. Louis, MO), unless otherwise specified. RP782, an ^{111}In-labeled tracer with specificity for activated MMPs [3] was provided by Lantheus Medical Imaging (North Billerica, MA).

Animal Model

Left common carotid injury was induced in apoE$^{-/-}$ mice (n=59) as previously described [4, 5]. Briefly, six to eight-week old female apoE$^{-/-}$ mice (Jackson Laboratory, Bar Harbor, Maine) were fed high-cholesterol (1.25% Cholesterol, Harlan) chow ad libitum. After 1 week, the common carotid and external carotid arteries were exposed by blunt-end dissection under anesthesia (ketamine 100 mg/kg, and xylazine 10 mg.kg, i.p.), and the left common carotid artery was injured with 6 passes of a 0.014" guide wire introduced through the external carotid artery. The opposite carotid artery was approached but not injured, and served as control. Buprenorphine (0.05 mg/kg, sc) was used for post-operative analgesia. Experiments were performed according to regulations of Yale University's Animal Care Committee.

Histology, morphometry, immunofluorescent (IF) and in situ zymography studies

Groups of 4 animals were anesthetized before and at 1, 2, 3, or 4 weeks after injury (supplemental figure 1). Following perfusion with normal saline, carotid arteries were harvested, embedded in OCT compound, snap-frozen, and stored at −80°C until further use. IF staining was performed using standard techniques on 5 μm thick, cryostat sections. Primary antibodies included anti-mouse MMP-2 and MMP-9 (Chemicon, Temecula, CA), smooth muscle α-actin (Sigma), and CD31 (BD Pharmingen, San Jose, CA). Isotype –matched antibodies were used as control. Nuclei were detected with DAPI. For morphometric analysis microscopic measurements were performed on cryostat sections at 250 μm below carotid bifurcation using NIH Image J software, as described [5]. Changes in morphometric indices were calculated by subtracting from measurements at any time point those of the preceding time point. MMP activation was assessed by in situ zymography. Frozen sections were placed on Zymo-film (Wako, Richmond, VA), and incubated at room temperature for 3 minutes. The film was then immersed in ponceau to stain the gelatin membrane. Protease activity was

manifested as a white area. Specificity for MMPs was be demonstrated in the presence of 1,10-phenanthrolone (PT), an MMP-inhibitor.

Imaging

For imaging experiments RP782 (11.1 MBq) was administered to groups of 5-7 animals at 1, 2, 3, and 4 weeks after injury through an inferior vena cava intravenous catheter. Animals were imaged after 2 hours using a dedicated high resolution small animal imaging system (X-SPECT, GammaMedica-Ideas), using one mm medium energy pinhole collimators. In micro-Jaszczak phantom studies, this system has a resolution of 0.8 and 2 mm for ^{99m}Tc and ^{111}In, respectively. Anesthetized mice (with isofluorane) were placed in a fixed position on the animal bed. A point source of known activity (~1 μCi) was placed in the field of view, but outside the body, to quantify uptake and to verify the accuracy of image fusions. MicroSPECT imaging was performed in a step and shoot manner, using the following acquisition parameters: 64 projections, 30 seconds/projection (~35 minute image acquisition), 174 and 242 keV photopeaks ± 10% window. After completion of microSPECT imaging animals were injected with a continuous infusion of iodinated CT contrast (Omnipaque, 100μl/mn) over 2 minutes and CT imaging was performed (energy: 75 kV/280 uA, matrix: 512×512) to identify anatomical structure. The imaging protocol lasted ~ 1 hour, after which (3 hours after tracer administration) different tissues were harvested for gamma counting and autoradiography. MicroSPECT images were reconstructed through iterative reconstruction (5 iterations, 4 subsets) using system software (FLEX SPECT, GammaMedica Ideas). CT projection images were reconstructed using commercial software (Cobra, Exxim Computing Corp., Pleasanton, CA), that implement a cone-beam reconstruction algorithm. Reconstructed microSPECT images were reoriented according to the CT anatomical images, fused, and exported in the Interfile format for further processing using Amide Medical Imaging Data Examiner [6]. When necessary, image fusion was manually adjusted with the help of a fiducial marker and anatomical landmarks. For quantitative analysis of tracer uptake cylindrical regions of interest (ROIs) were drawn at the level of carotid artery bifurcation (2 × 2 × 2 mm). A ROI immediately posterior to both carotids (1 × 1 × 1 mm) served as background.

Autoradiography

After imaging, carotids were harvested for autoradiography at three hours post-tracer administration (n=24). An additional group of animals (n=12) were used for autoradiography and biodistribution studies at 6 hours. Blocking experiments were performed at 6 hours in 3 animals in the presence of 50-fold excess non-labeled RP782 which was administered 5 minutes prior to RP782 administration. Samples were exposed to high sensitivity x-radiographic X-OMAT Kodak Scientific Imaging Film (Eastman Kodak, Rochester, NY) for various times to optimize detection. Tracer uptake was quantified by quantitative autoradiography using a standard curve, and expressed as mBq/pixel. Background corrected signal intensities in the regions of interest were measured on high resolution images using 1D Image Analysis Software. A standard curve was derived from a series of standards with known activity deposited on Whatman paper and exposed to the same film. Multiple exposures for each film were obtained, the linear range determined and utilized for quantitative analysis of tracer uptake in the target artery.

Gamma counting

Samples were weighed and gamma counting was performed on a gamma counter (Cobra, Perkin-Elmer, Shelton, CT). The values were background, decay and weight corrected.

Assay for activated MMP specificity

Five μm thick sections of the left carotid artery at 3 weeks post-injury were exposed to PT, a broad spectrum MMP-inhibitor (10mM, Invitrogen, San Diego, CA) or control buffer for 10 minutes at 37°C. Next, RP782 (3.7 kBq) was added for 20 minutes, samples were washed for three times, and the tissue was transferred to a tube for gamma counting.

Statistical analysis

All data are presented as mean value ± standard deviation. Morphometric data and tracer uptake specificity were analyzed by Mann Whitney test. Paired t-test after logarithmic transformation (ratio t-test) was used to examine the statistical significance of the difference in tracer uptake between right and left carotid arteries. The non-parametric Spearman's correlation was used to test the association between two variables. Significance was set at the 0.05 level.

The authors had full access to the data and take responsibility for its integrity. All authors have read and agree to the manuscript as written.

Results

Matrix Metalloproteinase Activation in Vascular Remodeling

We used an established model of wire injury to the arterial wall in apolipoprotein (apo)$E^{-/-}$ mice as the prototypic example of vascular remodeling. Left common carotid artery injury led to significant vessel wall hyperplasia and expansive remodeling over a period of four weeks (figure 1). The left carotid artery neointima and media area increased from 12,677 ± 2424 μm^2 before injury to 176,352 ± 14,198 μm^2 at 4 weeks after injury (n=4, p=0.028). Concomitantly, there was a compensatory enlargement of the artery, with the total cross-sectional vessel area increasing from 75,354 ± 22,180 μm^2 in non-injured arteries, to 206,541 ± 18,336 μm^2 at 4 weeks after injury (p=0.028). Over the same period of time, the cross sectional luminal area decreased from 62677 ± 21841 μm^2 to 30189 ± 17289 μm^2 (p= 0.057). Although partial ligation of the carotid artery can potentially lead to changes in flow and structural changes in the contralateral artery [7], the morphometry of the sham-operated right common carotid artery remained unchanged from baseline.

MMP-2 and -9 play a key role in vascular remodeling [2]. Therefore, we focused our ex vivo studies of vascular remodeling on these two members of the MMP family. Immunostaining of sham-operated carotid arteries demonstrated little constitutive MMP-2 and MMP-9 expression, predominantly confined to the media. Concomitant with the changes in the vessel size and composition in response to wire injury, there was a marked increase in MMP-2 and -9 expression levels, which was detectable at 1 week and peaked at two to three weeks after injury (figure 2). Co-immunostaining with cell-specific markers demonstrated MMP-2 co-localization with α-actin positive vascular smooth muscle cells (VSMCs) and CD31 positive endothelial cells (ECs, figure 3). MMP-9 co-localized with α-actin positive VSMCs (not shown).

Next, we assessed the MMP-2 and -9 protease activity by in situ gelatinase zymography in normal and injured carotid arteries. Despite the constitutive MMP-2 (and to a lesser degree MMP-9) expression, we did not detect any gelatinase activity in normal carotid arteries (figure 4). Wire injury led to an increase in gelatinase activity which was detectable as early as one week after injury and become more prominent by three weeks. The MMP-specificity of this gelatinase activity was demonstrated by the marked reduction in proteolysis in the presence of a specific MMP-inhibitor, 1,10-phenanthrolone (PT).

MicroSPECT/CT Imaging of MMP Activation in Vascular Remodeling

As a prelude to imaging studies, we addressed the biodistribution of RP782, a novel ^{111}In-labeled tracer which specificity targets activated MMPs [3], in apoE$^{-/-}$ mice. Tissue uptake was quantified by gamma well counting at 3 and 6 hours (n=3 in each group) after intravenous administration of the tracer (11.1 MBq), and demonstrated rapid renal clearance and favorable pharmacokinetics for in vivo imaging (supplemental figure 2). The blood pool activity was 2.5% ± 0.4% and 0.2% ± 0.0% injected dose (ID)/g respectively, at 3 and 6 hours. Due to the small size of carotid arteries, their weights could not be accurately measured. We used morphometric estimates of the carotid artery volume to assess carotid artery to blood uptake ratio (3.3 ± 1.6 for the right carotid and 11.9 ± 6.1 for the injured left carotid artery at three hours, n=6 two to four weeks after surgery, p=0.004).

Next, we used a hybrid microSPECT/CT system to image MMP activation and localize it to remodeling murine arteries identified by angiography. RP782 (11.1 MBq) was administered to apoE$^{-/-}$ mice (n=24) at 1, 2, 3, and 4 weeks after left common carotid artery injury. MicroSPECT imaging was started at 2 hours post-injection, and was followed by CT angiography to localize carotid arteries. Tracer uptake in injured carotid arteries was visually detectable on microSPECT/CT images at 2, 3, and 4 weeks after injury (figure 5a, b, c and supplemental movie). Quantitative analysis of image-derived tracer uptake demonstrated a significant difference in target to background activity between the injured left, and control right carotid arteries (1.62 ± 0.36 and 1.29 ± 0.20 for left and right carotid arteries, $p<0.0001$). Background-corrected tracer uptake in the injured left carotid artery was significantly higher than uptake in the right carotid artery at two (p=0.004), and three (p=0.03) weeks after injury (fig 5d). In some of the animals, tracer uptake was also detectable at the surgical site.

Autoradiographic RP782 Uptake Quantitation and Specificity

RP782 uptake in carotid arteries was further assessed by quantitative autoradiography. Consistent with in vivo imaging results, tracer uptake was significantly higher in the injured, as compared to contra-lateral, control arteries. at all time points after injury with (fig 6a), with the uptake intensity increasing from 478 ± 337, 550 ± 356, 504 ± 118, and 642 ± 344 mBq/pixel in the non-injured right carotid to 1123 ± 475, 2389 ± 1013, 2093 ± 941, and 1946 ± 867 mBq/pixel in the injured left carotid artery at 1, 2, 3, and 4 weeks after injury (n=5 to 7 in each group, p=0.004 for the right carotid versus left carotid at 1 week, <0.001 at two, three, and four weeks) (figure 6b). Similar results were obtained when the carotid uptake was analyzed at 6 hours post injection (Data not shown).

RP782 uptake specificity was addressed in a group of animals at two to three weeks after carotid injury. Animals were pretreated with 50-fold excess non-labeled tracer. Six hours following RP782 administration (11.1 MBq), tracer uptake in the left carotid artery was markedly reduced in animals pretreated with excess non-labeled tracer demonstrating specificity of RP782 uptake (from 720 ± 255 to 44 ± 8 mBq/pixel, n=6 without and 3 with blocking, p=0.02) (figures 7a and 7b).

RP782 specificity for activated MMPs in the vessel wall was addressed on sections of the left carotid artery at three weeks after injury. A broad spectrum MMP inhibitor, PT (10mM), significantly inhibited RP782 binding to carotid artery (from 37.8 ± 40.4 to 4.1 ± 7.3 cpm per section, n=8, p=0.002), demonstrating activated MMP-specificity of RP782 binding (figure 7c).

Biological Significance of RP782 Uptake

MMP activation, detectable by RP782 imaging, plays a pivotal role in several aspects of vascular remodeling, including vascular cell proliferation/migration, as well as reorganization

of the matrix scaffold. To define the biological significance of RP782 uptake in injury-induced vascular remodeling, we assessed the correlation between morphometric indices of vascular remodeling, namely hyperplasia and expansive remodeling, and RP782 uptake. There was an excellent correlation between RP782 uptake and weekly changes in the vessel wall (neointima + media) cross-sectional area (Spearman's r=0.95, p=0.001) (figure 8), but not with changes in the total vessel (r= 0.59, p=0.13) or luminal (r= -0.09, p= 0.84) areas.

Discussion

In this study we demonstrated the feasibility of high sensitivity-high resolution microSPECT/CT molecular imaging of MMP activation in injury-induced vascular remodeling using a novel activated MMP-specific tracer. Furthermore, we established a potential application of imaging MMP activation in tracking vessel wall hyperplasia in vivo. Matrix metalloproteinases (MMPs) are a multi-gene family of at least 23 secreted or transmembrane zinc- and calcium-dependent endopeptidases that selectively digest individual components of the extracellular matrix (ECM). MMPs are biosynthesized either as secreted or transmembrane proenzymes. The secreted MMPs are released into the extracellular space in a latent or proenzyme state (pro-MMP). Activation of these latent MMPs is achieved through enzymatic cleavage of the propeptide domain. Activated MMPs degrade ECM (and other) proteins [8, 9] at highly specific peptide sequences [10]. In the normal blood vessel, MMPs are involved in maintaining the vessel's integrity by breaking down ECM while new matrix is being synthesized. Amongst many MMPs expressed in vascular tissue [11], MMP-2 and -9 [12-14] play an important role in vascular pathology. Normal arteries express MMP-2, TIMP-1 and TIMP-2, which are produced constitutively by ECs and VSMCs. However, there is no detectable in situ MMP enzymatic activity in normal arteries [2]. MMP activation is a key mediator of vascular remodeling. Vascular remodeling, a persistent change in a blood vessel size or composition, is a common feature of many vasculopathies, including atherosclerosis and aneurysm formation. ECs, VSMCs and inflammatory cells are the main sources of MMP production in vascular remodeling [2, 15].

The strength of molecular imaging in tracking molecular events is dependent on the development of highly specific probes which can be detected by an appropriate imaging technology [16]. In recent years, there has been considerable progress towards the development of novel molecular imaging approaches for detection of cancer [17-19]. However, applying the same concepts to vascular imaging has proved to be highly challenging [20]. The small size of the target (in the sub-mm range in mice) and immediate vicinity to the blood pool are major limiting factors for in vivo detection of molecular and cellular events in blood vessels. As such, vascular molecular imaging is highly dependent on the availability of high resolution, high sensitivity imaging systems. Light-based imaging modalities [21-24] are limited by the depth of penetration and are not (as yet) quantitative in vivo [25, 26]. Scintigraphic imaging can provide the high sensitivity required for in vivo imaging [19]. However, it is somewhat limited in the ability to localize the target signal to a specific anatomical structure [27-29]. An example of this limitation can be seen in a recent study on imaging MMP activation in ligated carotid arteries by planar imaging which could not discriminate the uptake in the surgical wound from that of the target artery [30]. Recent technological advances have somewhat improved this limitation of scintigraphic imaging (whether PET or SPECT) in regards to spatial resolution. Despite these improvements, identification of the target artery may only be achieved through concomitant use of high resolution CT angiography (or magnetic resonance imaging). This hybrid imaging approach enabled us to clearly identify the arterial tree and localize the RP782 signal to the injured carotid arteries, distinguishing it from the more superficial surgical wound uptake.

A number of MMP-targeted radiotracers have been developed and evaluated for imaging cancer [31-33], ventricular remodeling [3] and vascular pathology [30]. A common feature of these agents, and RP782 used in our study, is their broad spectrum of MMP targets [3]. While we have focused our evaluation of MMP activation on gelatinases, several other MMPs are involved in vascular pathology and may play an equally important role in vascular remodeling [2, 15]. Imaging specific members of the MMP family would be of great significance as a research tool. This is dependent on the development of novel, highly specific tracers, which may be based on the structure of specific inhibitors currently under development. It is uncertain whether broadly or more narrowly specific tracers will better serve as clinical diagnostic tools in specific situations such as vulnerable plaque and aneurysm rupture, where MMP activation plays a key role.

The two components of vascular remodeling, geometrical remodeling (expansive remodeling in the case of wire injury) and hyperplasia, play complementary, yet distinct, roles in vascular remodeling. MMPs are key mediators of vascular cell differentiation, migration, proliferation, and survival, as well as reorganization of the matrix scaffold. There are conflicting data on the biological significance of MMP-2 and -9 expression and activation in vascular remodeling. VSMC migration in the balloon-injured rat carotid artery is reduced by the administration of a non-selective MMP inhibitor, GM6001 [34, 35]. However, this inhibition is not associated with a reduction in the size of neointima. Adenoviral expression of TIMP-1 inhibits VSMC migration and neointima formation in the balloon-injured rat carotid artery [36]. MMP-9 over-expression in VSMCs leads to expansive remodeling and thinning of the intima in the rat carotid arteries [37], and geometrical remodeling and neointima formation induced by endothelial denudation or carotid ligation is reduced in MMP-2 and -9 knock out mouse [14, 38, 39]. There is a relative paucity of information on the activation state of MMPs in vascular remodeling. This is in part due to the absence of appropriate in vivo measures of MMP activation. The availability of an activation-specific MMP-targeted tracer provided us with the opportunity to track MMP activation in vivo. Given the active role of MMPs in the pathogenesis of vascular remodeling, it is reasonable to assume that MMP activation correlates with temporal changes in morphometric indices of vascular remodeling. Although both the expansive remodeling and neointima formation are dependent on MMP function, a significant correlation could be shown with changes in the neointima and media area (which parallels vascular cell proliferation [5]), but not changes in the total vessel area. This may indicate that MMP activation plays a more pivotal role in the hyperplastic response to injury, and that other non-MMP proteolytic systems, such as the plasminogen/plasmin system [15], are the predominant regulators of geometrical remodeling.

Clinical relevance

While valuable as an investigational tool for preclinical studies, MMP-targeted imaging also allows for tracking MMP activation in humans, MMP activation plays a key role in vascular morbidity and mortality [2]. Protease-mediated disruption of the thin fibrous cap of vulnerable plaque can lead to myocardial infarction and death, Similarly, MMP activation is a key mediator of aneurysm expansion and rupture. As such, MMP-targeted imaging may potentially identify high risk patients, e.g., those at risk for acute coronary syndromes or prone to aneurysm rupture. Neointimal hyperplasia is the predominant pathological feature in in-stent restenosis, graft arteriosclerosis, and diabetic vasculopathy. The ability to track vessel-wall hyperplasia non-invasively may lead to early detection, for example, in graft arteriosclerosis, which is often detected in the late stages when therapeutic interventions are not effective. Finally, given the causal role of MMP activation in pathogenesis, MMP-targeted imaging of vascular remodeling may provide a clinical tool to track the effect of therapeutic interventions in vascular disease.

Supplementary Material

Refer to Web version on PubMed Central for supplementary material.

Acknowledgements

We thank Dr. Barry Zaret for his valuable comments in preparing this manuscript.

Funding Sources: This work was supported by National Institutes of Health Program Project HL-70295, R01 HL85093, American Heart Association grant 0435053N and a Department of Veterans Affairs Merit Award to MMS.

References

1. Egeblad M, Werb Z. New functions for the matrix metalloproteinases in cancer progression. Nat Rev Cancer 2002;2:161–174. [PubMed: 11990853]
2. Galis ZS, Khatri JJ. Matrix metalloproteinases in vascular remodeling and atherogenesis: the good, the bad, and the ugly. Circ Res 2002;90:251–262. [PubMed: 11861412]
3. Su H, Spinale FG, Dobrucki LW, Song J, Hua J, Sweterlitsch S, Dione DP, Cavaliere P, Chow C, Bourke BN, Hu XY, Azure M, Yalamanchili P, Liu R, Cheesman EH, Robinson S, Edwards DS, Sinusas AJ. Noninvasive targeted imaging of matrix metalloproteinase activation in a murine model of postinfarction remodeling. Circulation 2005;112:3157–3167. [PubMed: 16275862]
4. De Geest B, Zhao Z, Collen D, Holvoet P. Effects of adenovirus-mediated human apo A-I gene transfer on neointima formation after endothelial denudation in apo E-deficient mice. Circulation 1997;96:4349–4356. [PubMed: 9416903]
5. Sadeghi MM, Krassilnikova S, Zhang J, Gharaei AA, Fassaei HR, Esmailzadeh L, Kooshkabadi A, Edwards S, Yalamanchili P, Harris TD, Sinusas AJ, Zaret BL, Bender JR. Detection of injury-induced vascular remodeling by targeting activated alphavbeta3 integrin in vivo. Circulation 2004;110:84–90. [PubMed: 15210600]
6. Loening AM, Gambhir SS. AMIDE: a free software tool for multimodality medical image analysis. Mol Imaging 2003;2:131–137. [PubMed: 14649056]
7. Korshunov VA, Berk BC. Flow-induced vascular remodeling in the mouse: a model for carotid intima-media thickening. Arterioscler Thromb Vasc Biol 2003;23:2185–2191. [PubMed: 14576075]
8. Gearing AJ, Beckett P, Christodoulou M, Churchill M, Clements J, Davidson AH, Drummond AH, Galloway WA, Gilbert R, Gordon JL, Leber TM, Managan M, Miller K, Nayee P, Owen K, Patel S, Thomas W, Wells G, Wood LM, Woolley K. Processing of tumour necrosis factor-alpha precursor by metalloproteinases. Nature 1994;370:555–557. [PubMed: 8052310]
9. Fernandez-Patron C, Radomski MW, Davidge ST. Vascular matrix metalloproteinase-2 cleaves big endothelin-1 yielding a novel vasoconstrictor. Circ Res 1999;85:906–911. [PubMed: 10559137]
10. Visse R, Nagase H. Matrix metalloproteinases and tissue inhibitors of metalloproteinases: structure, function, and biochemistry. Circ Res 2003;92:827–839. [PubMed: 12730128]
11. Newby AC. Dual role of matrix metalloproteinases (matrixins) in intimal thickening and atherosclerotic plaque rupture. Physiol Rev 2005;85:1–31. [PubMed: 15618476]
12. Kuzuya M, Iguchi A. Role of matrix metalloproteinases in vascular remodeling. J Atheroscler Thromb 2003;10:275–282. [PubMed: 14718744]
13. Lessner SM, Martinson DE, Galis ZS. Compensatory vascular remodeling during atherosclerotic lesion growth depends on matrix metalloproteinase-9 activity. Arterioscler Thromb Vasc Biol 2004;24:2123–2129. [PubMed: 15308548]
14. Johnson C, Galis ZS. Matrix metalloproteinase-2 and -9 differentially regulate smooth muscle cell migration and cell-mediated collagen organization. Arterioscler Thromb Vasc Biol 2004;24:54–60. [PubMed: 14551157]
15. Lijnen HR. Plasmin and matrix metalloproteinases in vascular remodeling. Thromb Haemost 2001;86:324–333. [PubMed: 11487021]
16. Jaffer FA, Weissleder R. Seeing within: molecular imaging of the cardiovascular system. Circ Res 2004;94:433–445. [PubMed: 15001542]

17. Gambhir SS. Molecular imaging of cancer with positron emission tomography. Nat Rev Cancer 2002;2:683–693. [PubMed: 12209157]
18. Blasberg RG. Molecular imaging and cancer. Mol Cancer Ther 2003;2:335–343. [PubMed: 12657729]
19. Blankenberg FG, Strauss HW. Nuclear medicine applications in molecular imaging. J Magn Reson Imaging 2002;16:352–361. [PubMed: 12353251]
20. Sadeghi MM. The pathobiology of the vessel wall: implications for imaging. J Nucl Cardiol 2006;13:402–414. [PubMed: 16750785]
21. Bremer C, Bredow S, Mahmood U, Weissleder R, Tung CH. Optical imaging of matrix metalloproteinase-2 activity in tumors: feasibility study in a mouse model. Radiology 2001;221:523–529. [PubMed: 11687699]
22. Bremer C, Tung CH, Weissleder R. In vivo molecular target assessment of matrix metalloproteinase inhibition. Nat Med 2001;7:743–748. [PubMed: 11385514]
23. Chen J, Tung CH, Allport JR, Chen S, Weissleder R, Huang PL. Near-infrared fluorescent imaging of matrix metalloproteinase activity after myocardial infarction. Circulation 2005;111:1800–1805. [PubMed: 15809374]
24. McIntyre JO, Fingleton B, Wells KS, Piston DW, Lynch CC, Gautam S, Matrisian LM. Development of a novel fluorogenic proteolytic beacon for in vivo detection and imaging of tumour-associated matrix metalloproteinase-7 activity. Biochem J 2004;377:617–628. [PubMed: 14556651]
25. Weissleder R. A clearer vision for in vivo imaging. Nat Biotechnol 2001;19:316–317. [PubMed: 11283581]
26. Massoud TF, Gambhir SS. Molecular imaging in living subjects: seeing fundamental biological processes in a new light. Genes Dev 2003;17:545–580. [PubMed: 12629038]
27. Elmaleh DR, Narula J, Babich JW, Petrov A, Fischman AJ, Khaw BA, Rapaport E, Zamecnik PC. Rapid noninvasive detection of experimental atherosclerotic lesions with novel 99mTc-labeled diadenosine tetraphosphates. Proc Natl Acad Sci U S A 1998;95:691–695. [PubMed: 9435254]
28. Tsimikas S, Palinski W, Halpern SE, Yeung DW, Curtiss LK, Witztum JL. Radiolabeled MDA2, an oxidation-specific, monoclonal antibody, identifies native atherosclerotic lesions in vivo. J Nucl Cardiol 1999;6:41–53. [PubMed: 10070840]
29. Khaw BA, Tekabe Y, Johnson LL. Imaging experimental atherosclerotic lesions in ApoE knockout mice: enhanced targeting with Z2D3-anti-DTPA bispecific antibody and 99mTc-labeled negatively charged polymers. J Nucl Med 2006;47:868–876. [PubMed: 16644758]
30. Schafers M, Riemann B, Kopka K, Breyholz HJ, Wagner S, Schafers KP, Law MP, Schober O, Levkau B. Scintigraphic imaging of matrix metalloproteinase activity in the arterial wall in vivo. Circulation 2004;109:2554–2559. [PubMed: 15123523]
31. Oltenfreiter R, Staelens L, Lejeune A, Dumont F, Frankenne F, Foidart JM, Slegers G. New radioiodinated carboxylic and hydroxamic matrix metalloproteinase inhibitor tracers as potential tumor imaging agents. Nucl Med Biol 2004;31:459–468. [PubMed: 15093816]
32. Medina OP, Kairemo K, Valtanen H, Kangasniemi A, Kaukinen S, Ahonen I, Permi P, Annila A, Sneck M, Holopainen JM, Karonen SL, Kinnunen PK, Koivunen E. Radionuclide imaging of tumor xenografts in mice using a gelatinase-targeting peptide. Anticancer Res 2005;25:33–42. [PubMed: 15816516]
33. Li WP, Anderson CJ. Imaging matrix metalloproteinase expression in tumors. Q J Nucl Med 2003;47:201–208. [PubMed: 12897711]
34. Bendeck MP, Zempo N, Clowes AW, Galardy RE, Reidy MA. Smooth muscle cell migration and matrix metalloproteinase expression after arterial injury in the rat. Circ Res 1994;75:539–545. [PubMed: 8062427]
35. Bendeck MP, Irvin C, Reidy MA. Inhibition of matrix metalloproteinase activity inhibits smooth muscle cell migration but not neointimal thickening after arterial injury. Circ Res 1996;78:38–43. [PubMed: 8603503]
36. Dollery CM, Humphries SE, McClelland A, Latchman DS, McEwan JR. Expression of tissue inhibitor of matrix metalloproteinases 1 by use of an adenoviral vector inhibits smooth muscle cell migration and reduces neointimal hyperplasia in the rat model of vascular balloon injury. Circulation 1999;99:3199–3205. [PubMed: 10377085]

37. Mason DP, Kenagy RD, Hasenstab D, Bowen-Pope DF, Seifert RA, Coats S, Hawkins SM, Clowes AW. Matrix metalloproteinase-9 overexpression enhances vascular smooth muscle cell migration and alters remodeling in the injured rat carotid artery. Circ Res 1999;85:1179–1185. [PubMed: 10590245]

38. Galis ZS, Johnson C, Godin D, Magid R, Shipley JM, Senior RM, Ivan E. Targeted disruption of the matrix metalloproteinase-9 gene impairs smooth muscle cell migration and geometrical arterial remodeling. Circ Res 2002;91:852–859. [PubMed: 12411401]

39. Cho A, Reidy MA. Matrix metalloproteinase-9 is necessary for the regulation of smooth muscle cell replication and migration after arterial injury. Circ Res 2002;91:845–851. [PubMed: 12411400]

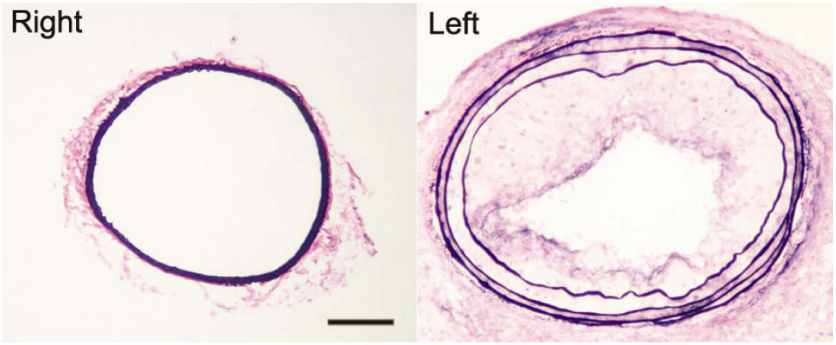

b

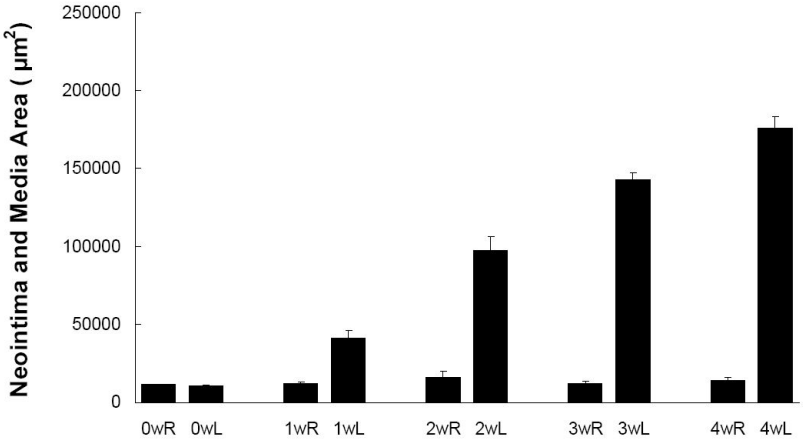

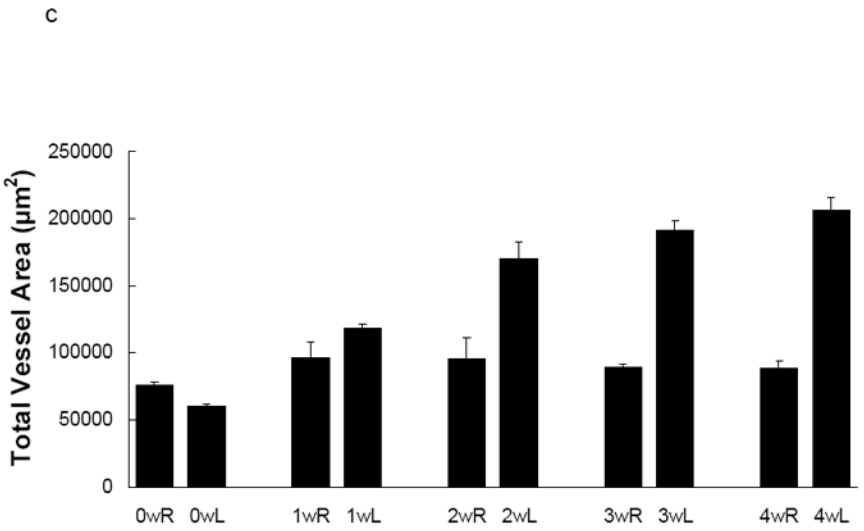

Fig 1.

a) Representative elastic van Giessen staining of the left common carotid artery in apoE$^{-/-}$ mouse in the absence (right) and 4 weeks following wire injury (left). Scale bar: 100 μm. b) Morphometric analysis of the media and intima, and c) total vessel area following left common carotid artery injury. n=4.

a

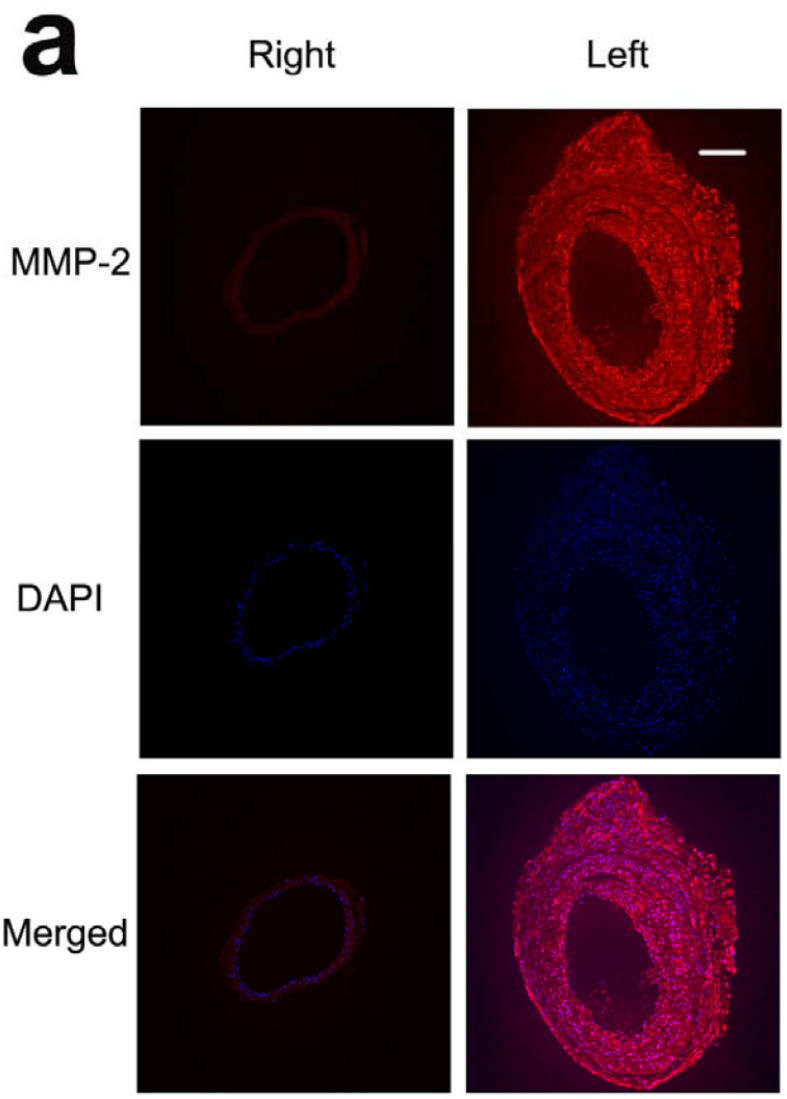

b

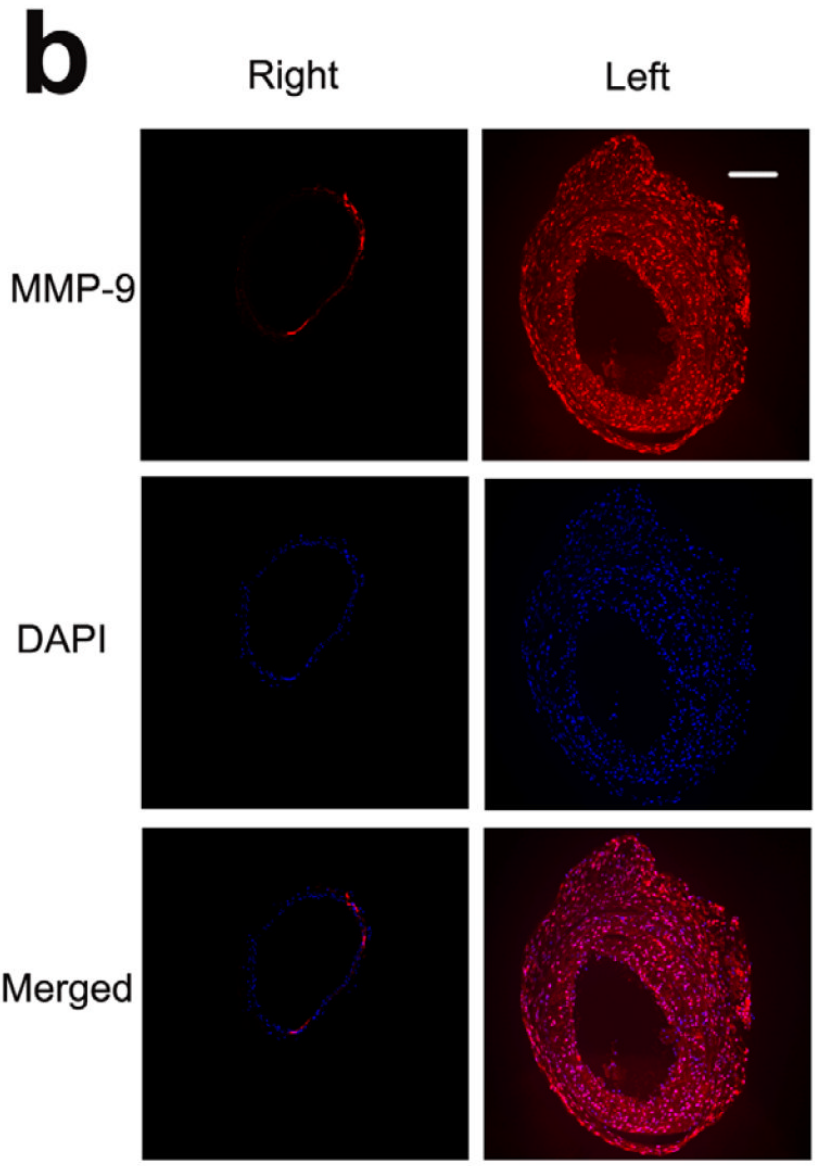

Fig 2.

Examples of MMP-2 (a) and MMP-9 (b) immunofluorescent staining of carotid arteries in non-injured right, and injured left arteries 3 weeks following wire injury, demonstrating increased MMP expression in response to injury. Scale bar: 100 μm. The figure is representative of three independent experiments.

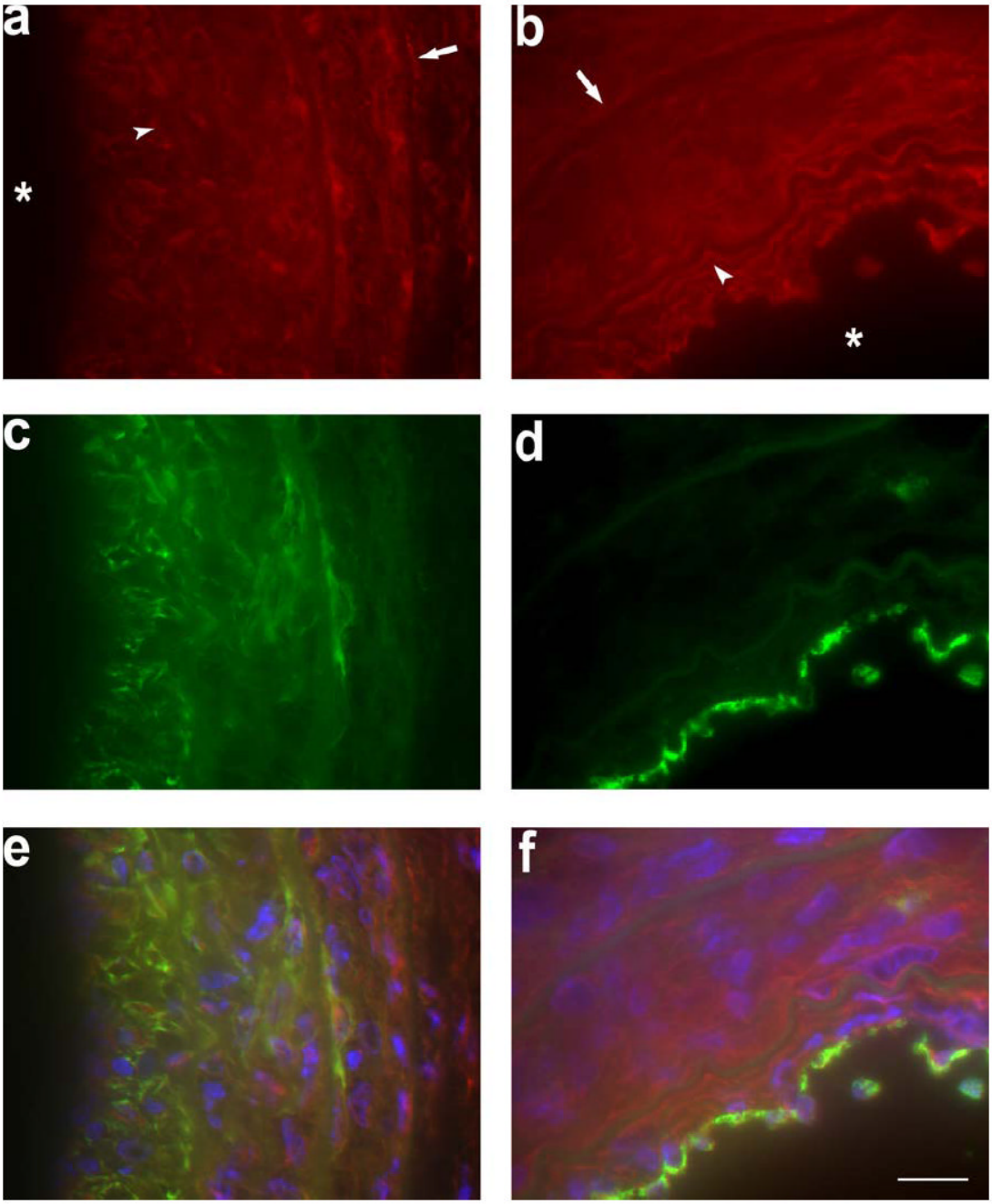

Fig 3.

Representative examples of MMP-2 (in red in a, b, e, and f) co-immunostaining with α-actin (in green in c and e) and CD31 (in green in d and f) in the injured left artery 2 weeks following wire injury. Yellow color on fused images (e and f) represents areas of co-localization, Nuclei are stained by DAPI in blue. Arrows and arrow heads point to external and internal elastic laminae, respectively. Stars mark the lumen. Scale bar: 10 μm.

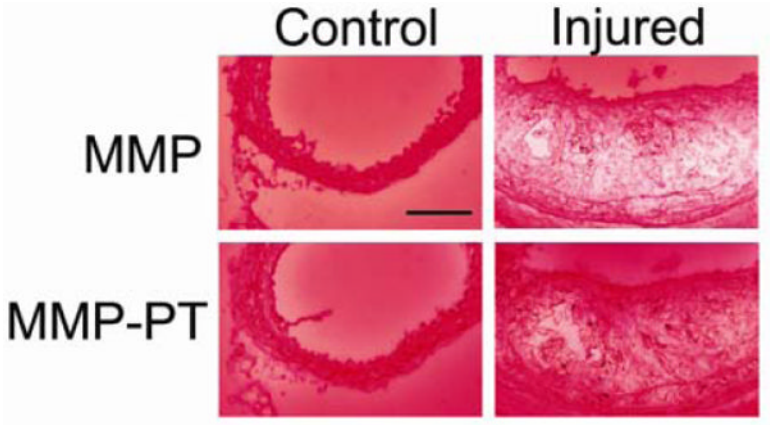

Fig 4.

Examples in situ gelatinase zymography of carotid arteries in the control right, and injured left arteries 3 weeks following wire injury, demonstrating increased gelatinase activation in response to injury. The bottom panels represent the gelatinase activity in the presence of an MMP inhibitor, 1,10-phenanthrolone (PT).Scale bar: 100 μm. The figure is representative of three independent experiments.

a b c

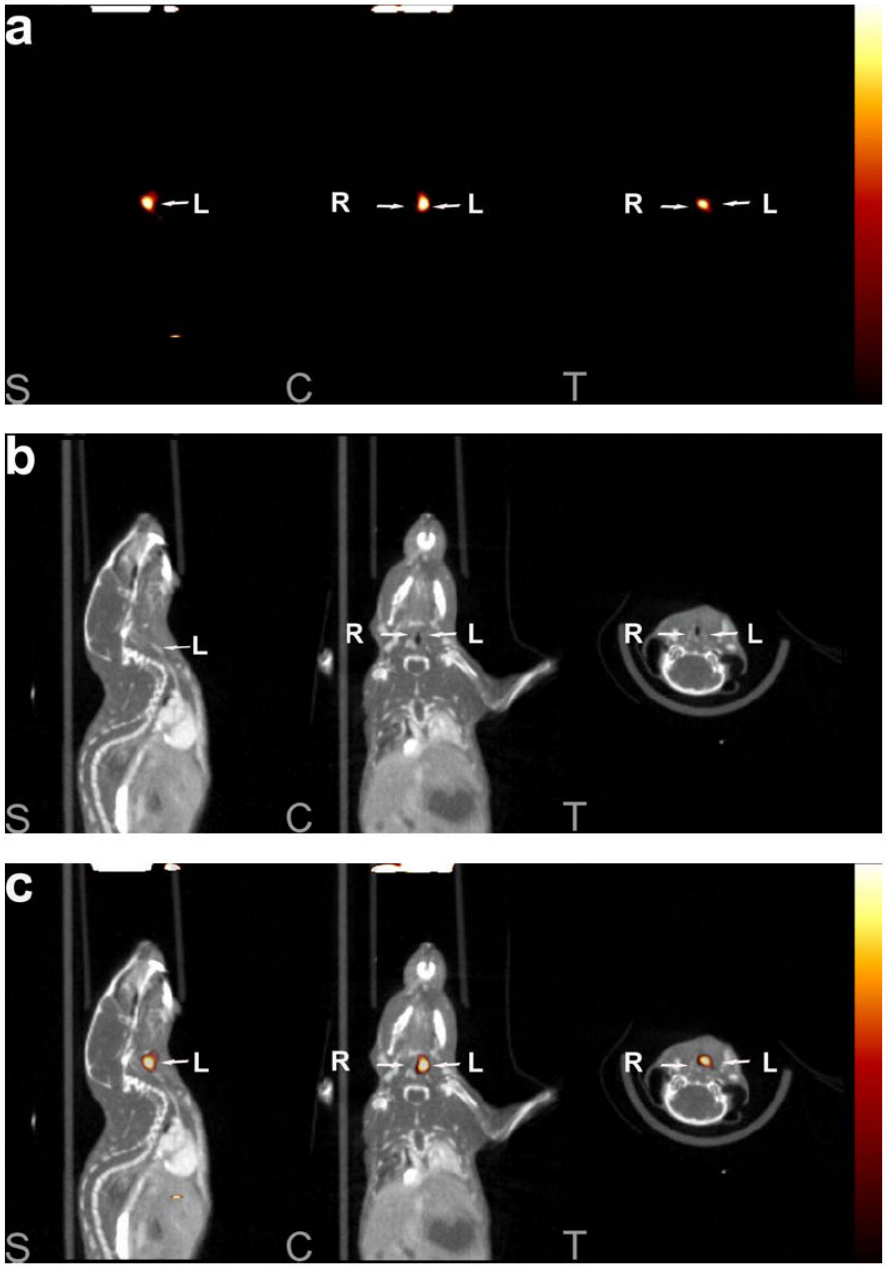

d

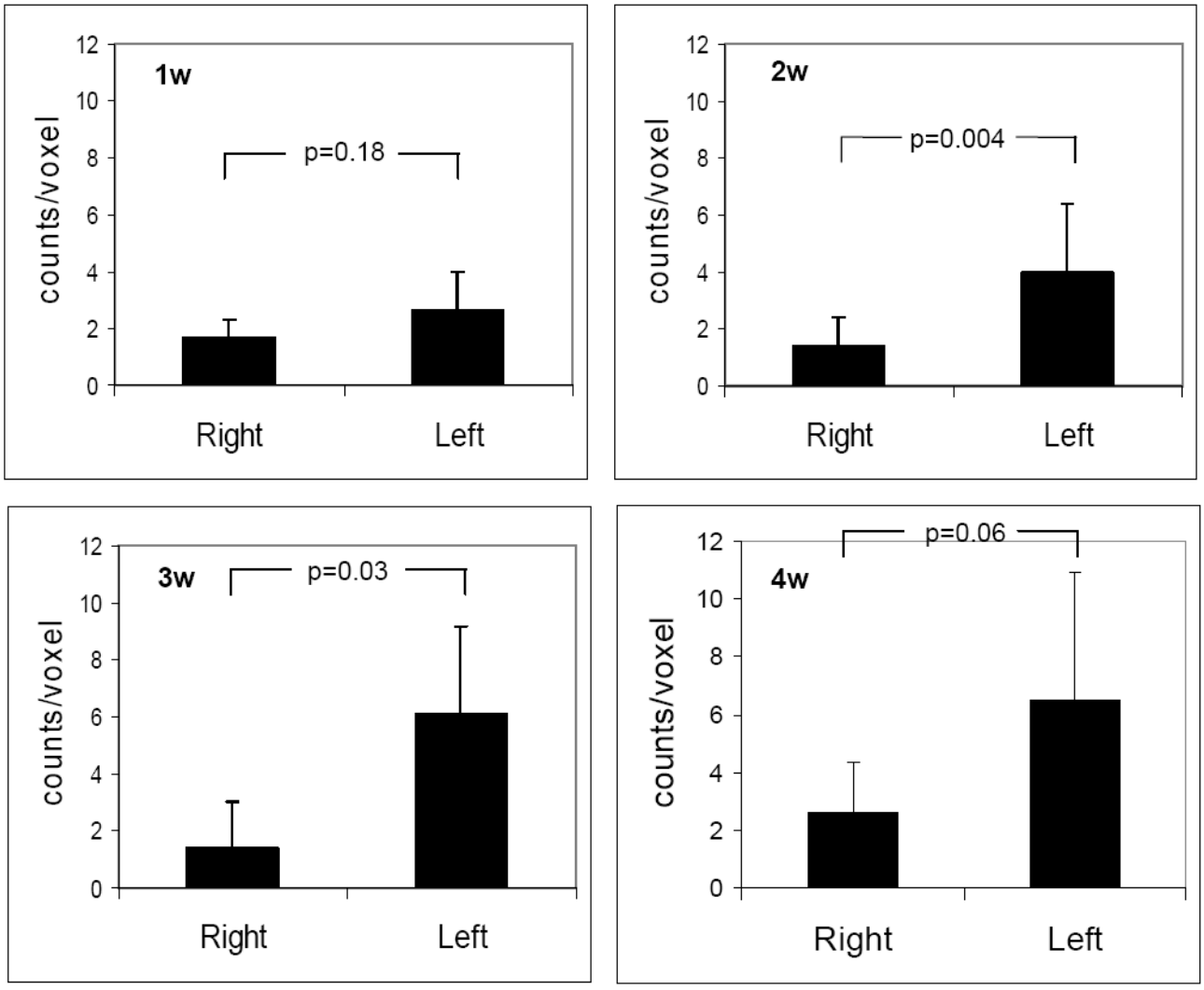

Fig 5.

An example of a) RP782 microSPECT, (b) CT angiography, and (c) fused microSPECT/CT in vivo imaging, at 3 weeks following carotid injury. Arrows point to the injured left (L) and non-injured right (R) carotid arteries. The small hot spot in the abdomen is likely the upper pole of the kidney on the edge of the SPECT field of view and/or a pinhole imaging artifact. S: sagittal, C: coronal, T: transverse slices. d) Image-derived quantitative analysis of background-corrected RP782 carotid uptake. n=5-7 in each group, w: week.

a

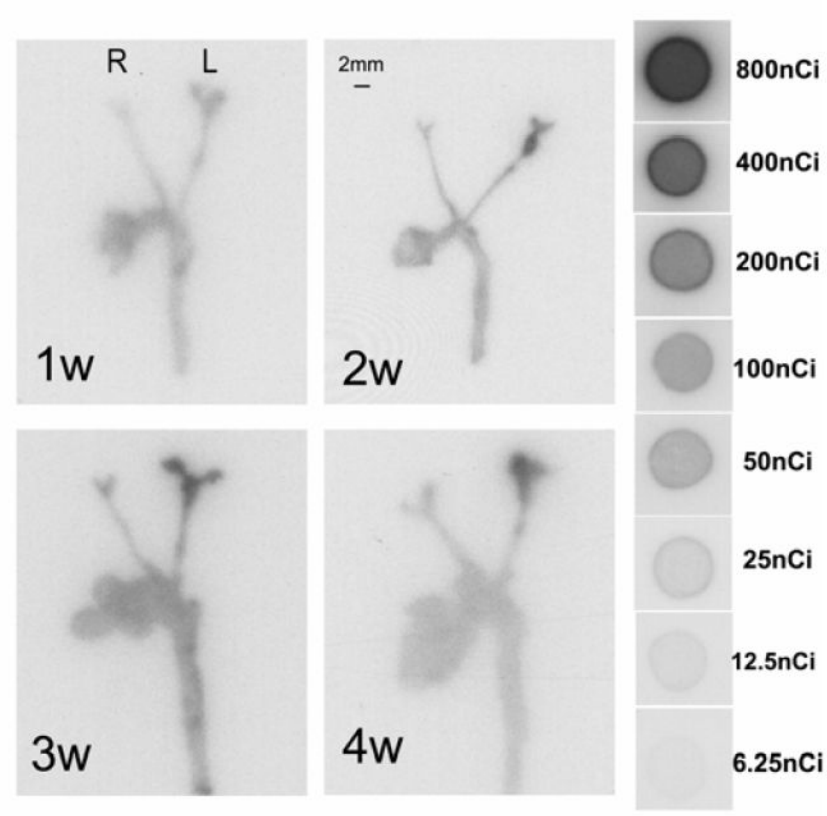

b

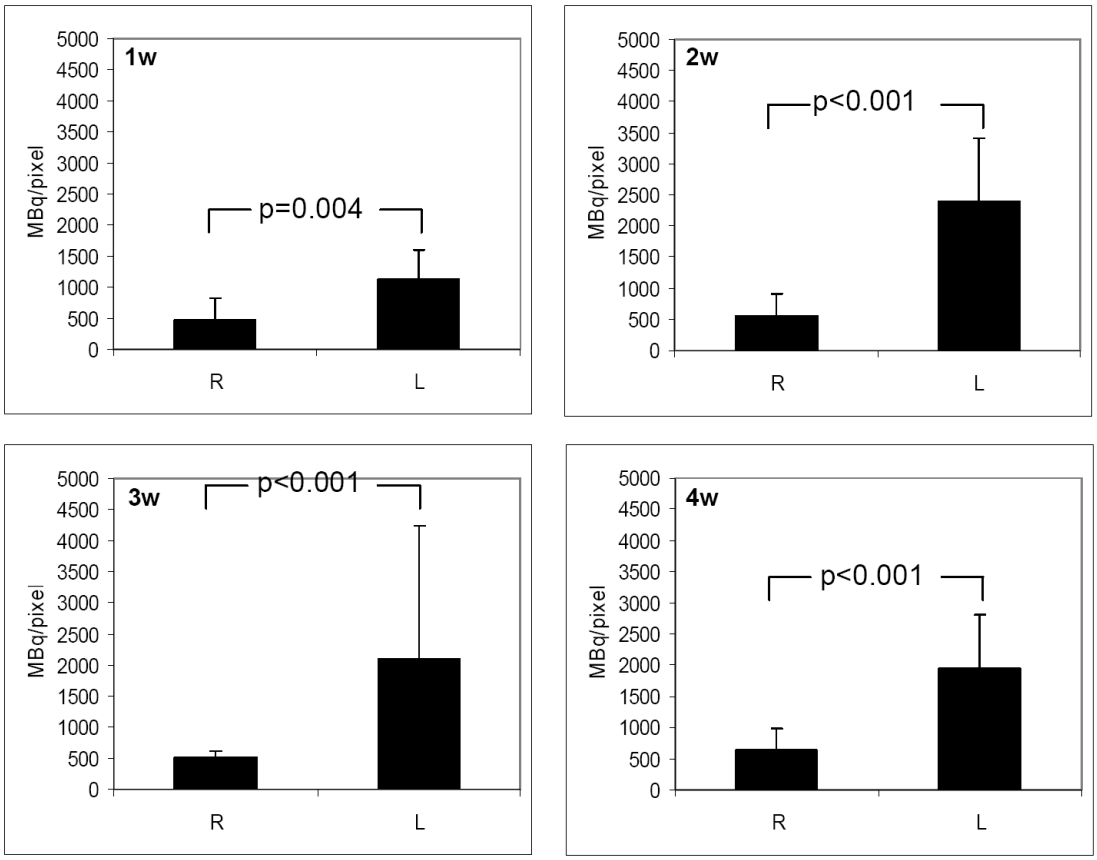

Fig 6.

a) Examples of quantitative carotid and aortic arch autoradiography at 1, 2, 3 and 4 weeks (w) following left common carotid injury three hours after RP782 administration, demonstrating significantly higher uptake of the tracer in the injured carotid artery as compared to uninjured right carotid artery. b) Quantitative autoradiography-derived measurement of RP782 uptake. n=5-7 in each group, L: Left, R: Right, scale bar: 2 mm.

a

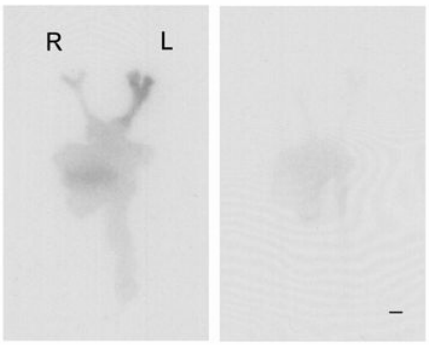

b

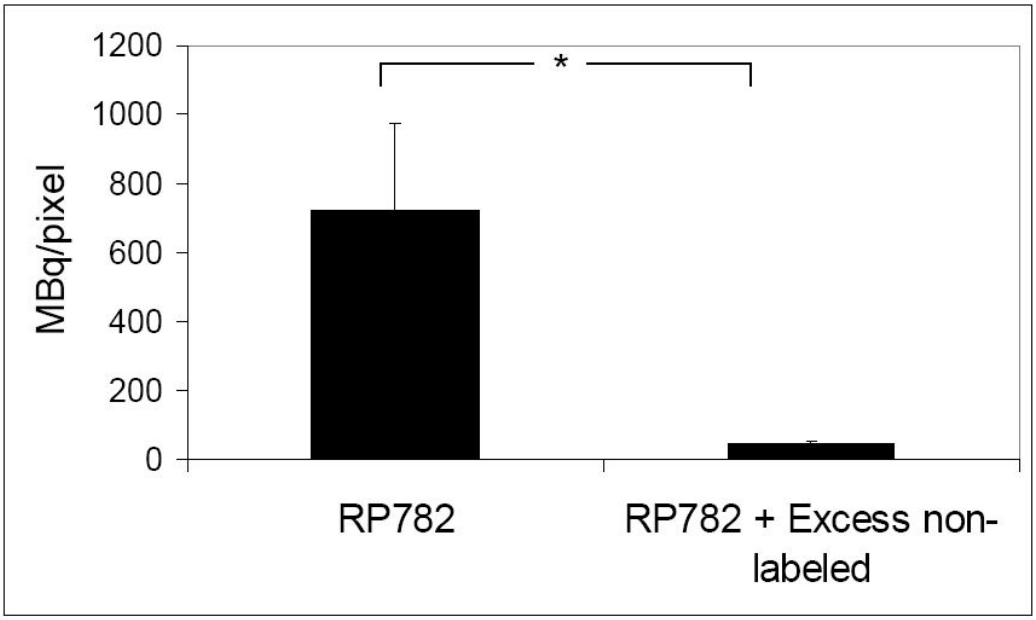

c

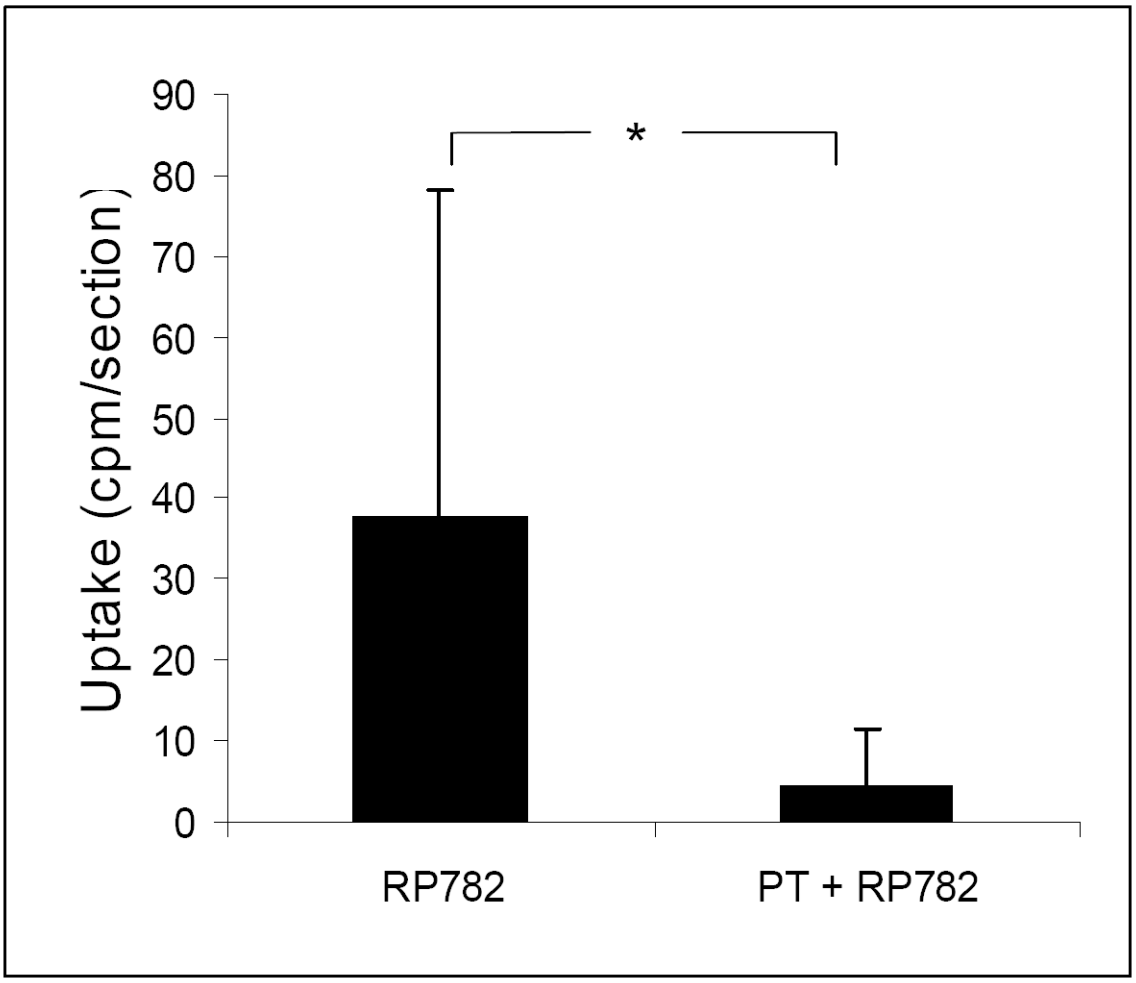

Fig 7.

a) Example of carotid artery and aortic arch RP782 autoradiography, in the absence (left) or presence of pretreatment with 50-fold excess non-labeled tracer (right) three weeks after left carotid wire injury, demonstrating marked reduction in tracer uptake after blocking with excess non-labeled tracer. L: Left, R: Right, scale bar: 2 mm. b) Quantitative autoradiography-derived measurement of RP782 uptake in the left carotid artery in the absence or presence of pretreatment with excess non-labeled tracer. n= 6 (without blocking) and 3 (with blocking), *: p=0.02. c) RP782 binding to section of the left carotid artery at three weeks after injury in the absence or presence of a broad spectrum MMP inhibitor 1,10-phenanthrolone (PT) assessed by gamma counting, demonstrating activated MMP-specificity of RP782 binding to the vessel wall. n=8, *: p=0.002, cpm: count per minute.

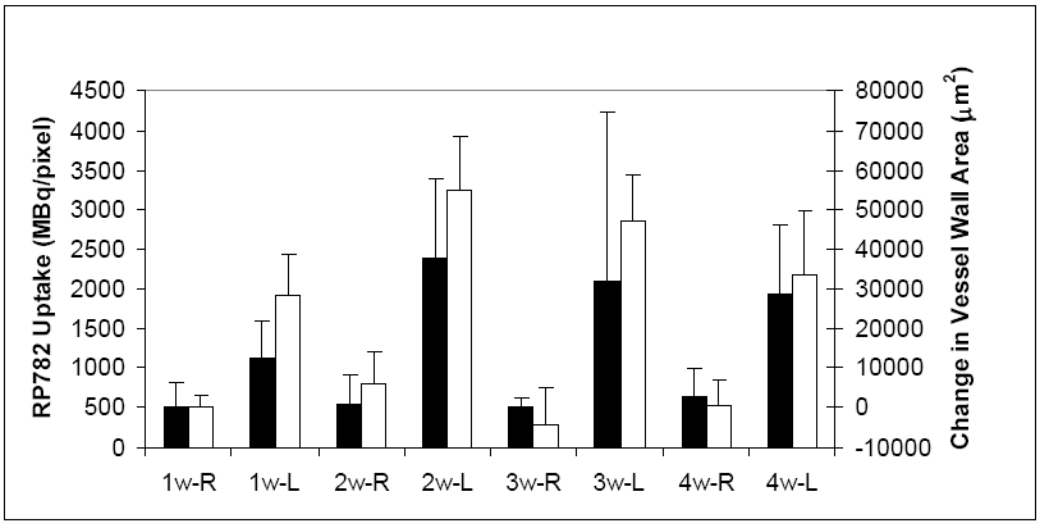

Fig 8.

Correlation between RP782 uptake (black bars) and weekly changes in the cross-sectional vessel wall (neointima + media) area (open bars). Spearman's R=0.95, p=0.001. w: week, R: right, L: left.